Raman Spectroscopic Studies of the Packing Properties of Mixed Dihexadecyl- and Dipalmitoylphosphatidylcholine Bilayer Dispersions

Mark T. Devlin and Ira W. Levin*

Laboratory of Chemical Physics, National Institute of Diabetes and Digestive and Kidney Diseases, National Institutes of Health, Bethesda, Maryland 20892

Received December 12, 1988; Revised Manuscript Received July 6, 1989

ABSTRACT: X-ray diffraction studies suggest the existence of two separate gel phases for mixed dihexadecylphosphatidylcholine (DHPC)/dipalmitoylphosphatidylcholine (DPPC) bilayers [Kim, J. T., Mattai, J., & Shipley, G. G. (1987) *Biochemistry 26*, 6599–6603; Lohner, K., Schuster, A., Degovics, G., Müller, K., & Laggner, P. (1987) *Chem. Phys. Lipids 44*, 61–70]. In one gel phase the lipid chains are interdigitated, while the other gel phase exhibits the conventional bilayer form. We use Raman spectroscopy to provide a detailed molecular analysis of the intermolecular and intramolecular interactions of the DHPC and DPPC molecules within these mixed bilayers. Observation of the methylene chain C–H stretching modes of DHPC and the methylene chain C–D stretching modes of DPPC-d_{62} for various mixed DHPC/DPPC-d_{62} bilayers enables the packing characteristics and conformational order of each lipid to be monitored separately. The spectral data indicate that the packing properties of DPPC-d_{62} in the mixed-lipid bilayers remain relatively unchanged, while the intramolecular and intermolecular properties of DHPC change dramatically as a function of the composition of the DHPC/DPPC-d_{62} mixed bilayer. This is consistent with a model based upon the existence of three characteristic lipid types for the mixed-lipid system, namely, domains of pure DPPC-d_{62} and pure DHPC species with interface lipids or boundary regions between the bulk domains.

Although ether-linked phospholipids exist in various mammalian tissues, the effects of these lipids on membrane properties have not been fully determined (Mangold & Paltauf, 1983; Albert & Anderson, 1977; Gross, 1984; Goldfine et al., 1987). In order to resolve more completely the structural and dynamical roles of ether-linked phospholipids, the physical properties of these lipids in model bilayers have been studied. In particular, dihexadecylphosphatidylcholine (DHPC), the ether-linked analogue of dipalmitoylphosphatidylcholine (DPPC), has been found to form subgel, gel, ripple, and liquid-crystalline phases similar to the lamellar phases formed by DPPC (Ruocco et al., 1985; Kim et al., 1987b; Laggner et al., 1987). DHPC also forms an interdigitated chain gel phase under high hydration conditions ($>\sim$30 wt % H_2O) below the bilayer pretransition. The main gel to liquid-crystalline phase transition temperature for DHPC is several degrees higher than the analogous phase transition temperature of DPPC (Ruocco et al., 1985; Kim et al., 1987b; Laggner et al., 1987). Additionally, differential scanning calorimetry (DSC) shows that DHPC/DPPC model bilayers have a single gel to liquid-crystalline phase transition whose enthalpy and temperature vary linearly with the composition of the DHPC/DPPC bilayer (Kim et al., 1987a; Lohner et al., 1987). These results imply that DHPC and DPPC are miscible and that no lateral separation occurs in these model bilayers. The complementary X-ray data indicate, however, that below the pretransition two gel phases may coexist in DHPC/DPPC model bilayers (Kim et al., 1987a). At 22 °C, DHPC/DPPC systems with <28 mol % DPPC exhibit lamellar periodicities of 47–49 Å, indicative of an interdigitated bilayer gel phase, while multilayers with >30 mol % DPPC have increased lamellar periodicities of 64–66 Å, indicative of a noninterdigitated bilayer gel phase. The DHPC/DPPC multilamellar system with 28 mol % DPPC gives two lamellar periodicities of 48.5 and 68.0 Å, denoting the coexistence of both interdigitated and noninterdigitated gel phases. For DHPC/DPPC mixtures in the ripple phase, Lohner et al. (1987) show a discontinuity in the bilayer repeat distance at 50 mol % DHPC. This suggests the existence of two separate ripple phases in DHPC/DPPC mixtures and may indicate a sample composition dependence on the lipid packing characteristics of these phases (Lohner et al., 1987).

To understand more fully the role of ether-linked phospholipids in binary mixtures and to specify their predominant interchain interactions and intrachain conformational changes, we examine in the present study the DHPC/DPPC mixed-lipid system by vibrational Raman spectroscopy. In particular, the Raman methylene stretching mode region sensitively reflects both inter- and intrachain interactions as a function of temperature and state of the binary mixtures (Levin, 1984). In order to examine independently the dynamical and conformational behavior of DHPC and DPPC in a mixture, we use a DPPC species whose acyl chains are completely deuterated (DPPC-d_{62}). Although chain-deuterated analogues have lower gel to liquid-crystalline phase transition temperatures than the nondeuterated species (Petersen et al., 1975), the packing, conformational, and dynamical properties of the deuterated and nondeuterated lipids are similar (Mendelsohn et al., 1976). More importantly, for DPPC-d_{62} the methylene chain C–D stretching mode region, extending from $\sim$2000 to 2300 cm^{-1} (as compared to the 2800–3100-cm^{-1} methylene chain C–H stretching mode region), is unoccluded by other vibrations from either the DPPC-d_{62} or DHPC species. Therefore, the packing dynamics of both DHPC and DPPC-d_{62} can be monitored separately in a mixed bilayer. The utility of this type of isotopic analysis has been previously demonstrated for a variety of bilayer systems (Laroche et al., 1988; Kouaouchi et al., 1985; Mendelsohn & Maisano, 1978; Mendelsohn & Taraschi, 1978).

The vibrational Raman spectra of the DHPC/DPPC-d_{62} binary mixtures allow a distinction to be made between either

* Address correspondence to this author at Room B1-27, Building 2, NIH, Bethesda, MD 20892.

Table I: Transition Temperatures (T_m) and Widths (ΔT) Determined from Calorimetric and Raman Spectroscopic Data[a]

sample	% DHPC	% DPPC-d_{62}		DSC[b]	DHPC[c] 2850/2880	DHPC[c] 2935/2880	DPPC-d_{62}[d] $\Delta\nu_{7/8}$	DPPC-d_{62}[d] $\Delta\nu_{1/2}$
DHPC	100	0	T_m	44.3 ± 0.1	41.8 ± 0.1	41.8 ± 0.1		
			ΔT	0.8 ± 0.1	1.2 ± 0.4	0.9 ± 0.2		
1	79	21	T_m	41.7 ± 0.1	39.9 ± 0.3	39.8 ± 0.2	*e*	38.9 ± 1.3
			ΔT	1.9 ± 0.1	2.0 ± 1.1	2.3 ± 0.6	*e*	9.5 ± 4.3
2	72	28	T_m	41.2 ± 0.1	40.0 ± 0.4	40.1 ± 0.1	41.2 ± 0.9	39.5 ± 0.3
			ΔT	2.0 ± 0.1	2.4 ± 1.1	2.9 ± 0.4	4.8 ± 2.8	1.2 ± 1.1
3	62	38	T_m	40.3 ± 0.1	37.7 ± 0.4	37.8 ± 0.1	38.3 ± 0.7	37.7 ± 0.4
			ΔT	3.4 ± 0.1	2.8 ± 1.2	2.4 ± 0.4	9.0 ± 2.4	3.7 ± 1.3
4	51	49	T_m	39.4 ± 0.1	35.3 ± 1.1	37.4 ± 0.3	38.4 ± 0.9	37.2 ± 1.1
			ΔT	3.4 ± 0.1	12.2 ± 3.9	3.0 ± 1.1	2.0 ± 2.7	5.1 ± 3.5
5	39	61	T_m	38.7 ± 0.1	36.1 ± 0.6	37.2 ± 0.3	36.5 ± 0.7	37.1 ± 0.5
			ΔT	3.0 ± 0.1	3.2 ± 2.3	1.8 ± 1.1	4.2 ± 2.6	3.7 ± 1.7
6	19	81	T_m	37.4 ± 0.1	34.5 ± 1.2	34.7 ± 0.4	35.2 ± 0.8	35.2 ± 0.2
			ΔT	2.7 ± 0.1	4.1 ± 3.9	2.0 ± 1.1	2.6 ± 2.6	2.4 ± 0.7
7	11	89	T_m	36.7 ± 0.1	*f*	33.1 ± 1.2	35.1 ± 0.4	34.8 ± 0.3
			ΔT	2.2 ± 0.1	*f*	6.1 ± 2.9	1.9 ± 1.3	3.2 ± 0.9
DPPC-d_{62}	0	100	T_m	36.1 ± 0.1			34.9 ± 0.9	34.7 ± 0.3
			ΔT	1.5 ± 0.1			4.2 ± 3.2	1.1 ± 1.1

[a] Errors associated with the values in this table are the 95% confidence limits of each value as determined from a Student's *t* distribution. [b] Transition temperatures determined from the calorimetric data. [c] Transition temperatures and phase transition widths determined from temperature profiles constructed from Raman spectra of the C–H stretches of DHPC. The 2850/2880 data reflect intermolecular changes in DHPC domains, and the 2935/2880 data reflect intramolecular changes in DHPC domains. See Materials and Methods for more details. [d] Transition temperatures and phase transition widths determined from temperature profiles constructed from Raman spectra of the C–D stretches of DPPC-d_{62}. The $\Delta\nu_{7/8}$ data reflect intermolecular changes in DPPC-d_{62} domains, and the $\Delta\nu_{1/2}$ data reflect intramolecular changes in DPPC-d_{62} domains. See Materials and Methods for more details. [e] Transition temperature and width of phase transition not reported since only two data points appeared in the transition region. As a result, the transition temperature and phase transition width were not varied in the nonlinear least-squares fitting procedure. [f] Transition temperature and width of phase transition not determined since no phase transition occurred.

the formation of pools of one set of lipid species, namely, domain formation, or complete miscibility of the two lipid species. For randomly distributed lipids, as suggested by DSC data (Kim et al., 1987a; Lohner et al., 1987), the Raman spectra would reflect similar DHPC and DPPC-d_{62} packing and dynamical properties. That is, the spectral data from both bilayer species would individually reflect the same phase transition behavior, and this behavior would be independent of the composition of the mixed bilayer, with the exception of variations in the phase transition temperature. If, however, DHPC and DPPC-d_{62} partition themselves into domains, different molecular dynamics and packing modifications should be spectroscopically observed for each lipid, with these bilayer alterations varying with changes in bilayer composition.

Materials and Methods

1,2-Di-*O*-hexadecyl-DL-phosphatidylcholine (DHPC) was purchased from Sigma Chemical Co.; 1,2-dipalmitoyl-L-α-phosphatidylcholine with completely deuterated acyl chains (DPPC-d_{62}) was obtained from Avanti Polar-Lipids Inc. The lyophilized powders of these lipids were combined to form the sample mixtures listed in Table I. These mixtures were dissolved in chloroform and then dried in two steps. Excess chloroform was removed from the samples by passing a stream of nitrogen across the dissolved samples. The samples were then dried under vacuum for 24 h. Dried powders were stored at −14 °C, the temperature of our freezer, until either the Raman spectra or the DSC thermograms of the samples were determined. Samples of pure DHPC and DPPC-d_{62} were also prepared from the stock lipid samples and stored at −14 °C. Raman samples were packed into a capillary tube, hydrated with distilled water, and then cycled several times through the main lipid phase transitions. Cycling through the main phase transition ensures that the different racemates of DHPC present in the mixed bilayers are all packed similarly (Sakurai et al., 1983; Boyanov et al., 1983; Tenchov et al., 1984; Boyanov et al., 1986). This conclusion is confirmed by our calorimetric measurements discussed in the next paragraph. The capillary tubes were sealed, and the samples were centrifuged for 10 min, on an International Microcapillary Centrifuge Model MB, prior to the Raman spectral measurements. Mild centrifugation pellets the sample for ease in recording higher signal/noise Raman spectra. The detailed features of the Raman spectra of samples before and after centrifugation are identical; therefore, centrifugation neither perturbs the lipid packing of the mixed bilayers nor separates the deuterated and nondeuterated lipid species. For the calorimetric determinations, approximately 2–6 mg of the sample powders was weighed into an ampule prior to the addition of 20 μL of distilled water.

The calorimetric measurements were recorded on a computer-controlled Hart Scientific calorimeter comprised of the following attachments: a Model 3705 adiabatic controller, a Model 3706 temperature scan controller, a Model 1701 Microtherm analog multiplexer and preamplifier, and a Model 707 digital voltmeter. The thermograms for each sample were measured as functions of increasing and decreasing temperature. Scans were performed at a rate of 20 °C/h. Three ascending temperature scans and three descending temperature scans of each sample were measured in order to ensure that the samples were fully hydrated and to demonstrate the absence of hysteresis. The transition temperatures of each sample were determined from the thermograms of the third ascending temperature scan. Phase transition temperatures and widths were determined from the data by use of two-state model for lipid phase transitions (Kirchhoff & Levin, 1987). The absence in our calorimetric scans of hysteresis in the main phase transition of the racemic mixtures of DHPC and L-α-DPPC-d_{62} confirms the homogeneous mixing of the various racemates (Sakurai et al., 1983; Boyanov et al., 1983, 1986; Tenchov et al., 1984). That is, the D and L isomers of DHPC are packed in similar fashions in the mixed bilayers examined in this paper.

Raman spectra were measured on a Ramalog 6 spectrometer with holographic gratings interfaced to a PDP 11/23 data acquisition system. Raman scattering was induced by an argon ion coherent radiation Innova 100 laser yielding 150 mW of

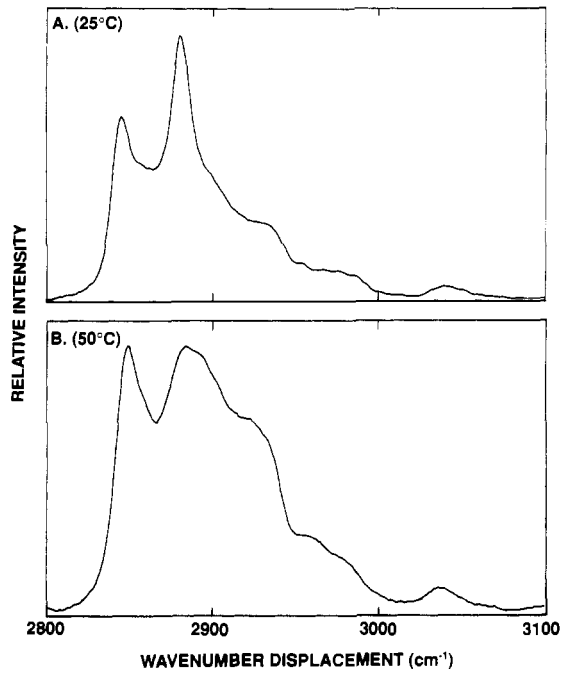

FIGURE 1: Raman spectra of the C–H stretching modes of pure DHPC bilayers in the gel phase [(A) 25 °C] and the liquid-crystalline phase [(B) 50 °C].

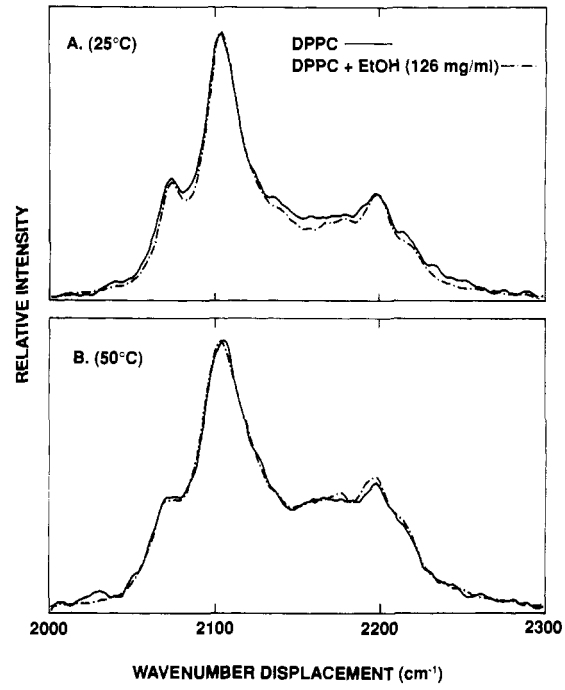

FIGURE 2: Raman spectra of the C–D stretching modes of pure DPPC-d_{62} bilayers in the gel phase [(A) 25 °C] and the liquid-crystalline phase [(B) 50 °C]. The solid lines represent the spectra of DPPC-d_{62} hydrated with distilled water, and the dashed lines represent the spectra of DPPC-d_{62} hydrated with 126 mg/mL ethanol. (The dashed-line spectrum in panel A is characteristic of interdigitated DPPC-d_{62} bilayers in the gel phase.)

power at the sample at 514.4 nm. Raman scattering from each sample was measured in the 2000–2300- and 2800–3100-cm^{-1} spectral regions. Spectra were obtained by signal averaging three scans recorded at a scan rate of 2 cm^{-1}/s with data collected every 1 cm^{-1}. The spectral resolution was 5 cm^{-1}. Sample temperatures were controlled by placing the sample capillary tubes in a brass block attached to a Neslab Endocal RTE-4 water bath. Changes in the Raman spectra of the samples were measured as a function of sample temperature. The water bath temperature, and thus the temperature of each sample, was varied by a Neslab ETP-4RC temperature programmer set to linearly increase the bath temperature at a rate of 1.5 °C/h. During the change in sample temperature, the Raman spectra were measured continuously. As a result, Raman spectra were collected at approximately 0.3 °C intervals. Temperature profiles of various Raman spectral parameters (see Results) were plotted against temperature and appropriately analyzed. Because of the large amount of spectral data required and the time involved in its acquisition, we sacrificed a small degree of sample local heating for increased Raman scattering. Although we limited the laser excitation power to 150 mW, we reduced the incident laser spot size to yield high signal/noise characteristics for signal averaging three scans. Two points are emphasized. In comparison to pure bilayer assemblies whose T_m's were determined by scanning calorimetry, the T_m's determined from our Raman data are reduced by about 2.5 °C. However, since the analysis of our spectral data is statistically robust, the precision of the temperature data, determined from Raman spectral parameters and listed in Table I, is high, and the comparisons made in Table I are statistically valid.

Results

Raman Spectral Order/Disorder Parameters for Lipid Bilayers. The Raman spectra of individual DHPC and DPPC-d_{62} components allow the molecular dynamics of the mixed DHPC/DPPC-d_{62} bilayer to be probed completely. Figures 1 and 2 depict the C–H and C–D stretching mode regions of DHPC and DPPC-d_{62}, respectively, in both the gel and liquid-crystalline phases. Although the band assignments, intensities, and frequency shifts have been previously reported and discussed (Levin, 1984; Bryant et al., 1982), a brief review of the salient vibrational parameters in these two spectral regions is necessary in order to discuss the molecular dynamics of the two lipids. In Figure 1A, three major Raman features are identified for the low-temperature gel phase of DHPC. The band at 2850 cm^{-1} corresponds to the methylene C–H symmetric stretching modes of the DHPC lipid chains. The methylene C–H asymmetric stretching modes assigned to the band at 2880 cm^{-1} lie [for the gel phase (Figure 1A)] on a background of methylene deformation overtones interacting with the methylene symmetric stretching fundamental modes. A Fermi resonance component of the chain terminal methyl C–H symmetric stretching mode, in addition to a Fermi resonance component involving the manifold of methylene deformation overtones, contributes to the band intensity in the 2935-cm^{-1} region. Since the C–H stretching modes of the choline headgroups of DPPC-d_{62} also contribute a small amount of intensity to the Raman bands in this region, appropriate corrections to the C–H stretching mode region of the mixed bilayers have been made. Other vibrational contributions to these bands have been described in detail elsewhere and will not be discussed here (Levin, 1984). In this context, it is important to identify frequency and intensity alterations in these bands as a function of temperature and as a change in the phase state of DHPC.

From a comparison of the gel phase (Figure 1A) and liquid-crystalline phase (Figure 1B) spectra of the DHPC bilayer, we note that, relative to the peak height intensity of the 2850-cm^{-1} band, the peak height intensities of the 2880- and 2935-cm^{-1} features decrease and increase, respectively. This is a consequence of the changes in Fermi resonsance effects between the methylene symmetric stretching modes and the manifold of overtone deformation modes. As the phase of the

bilayer changes, the separations between lipid chains and headgroup areas increase, along with an increase in the number of gauche conformers along the lipid chains. The loss of the predominantly all-trans nature of the lipid chains decreases the Fermi resonance coupling between the methylene deformation overtone modes and the symmetric methylene stretching modes, leading to the disappearance, in the liquid-crystalline phase, of the characteristic gel phase background centered around 2900 cm^{-1}. In addition, with the loss of symmetry of the lipid chains, infrared-active methylene asymmetric stretching modes become Raman active and contribute to the intensity and complexity of the 2935-cm^{-1} region (Bunow & Levin, 1977). These variations in the intensities and frequencies of the Raman bands reflect a response in the molecular vibrational energy levels to specific changes in the packing arrangements of the lipid bilayer. Increases in the spacing between lipid chains and concomitant reductions in lateral chain–chain interactions are monitored primarily by increases in the empirical peak height intensity ratio of the 2850- and 2880-cm^{-1} bands (I_{2850}/I_{2880}). Increases in the number of gauche isomers along the lipid chains, superimposed upon chain–chain interaction effects, are monitored by increases in the peak height intensity ratio I_{2935}/I_{2880} (Huang et al., 1982). Therefore, changes in DHPC bilayer dynamics and lipid packing properties can be determined from temperature profiles of these peak height intensity parameters.

In determining bilayer inter- and intramolecular disorder from the C–D stretching mode region, the analysis becomes more complicated. Figure 2 displays the C–D stretching region of the gel and liquid-crystalline phases of DPPC-d_{62} (solid lines). Although there are several Raman bands present in this spectral region, we concentrate our attention on two of these bands, namely, the feature at ~2075 cm^{-1}, corresponding to one Fermi resonance component of the acyl chain terminal methyl (CD_3) symmetric stretching mode, and the intense band at 2103 cm^{-1}, corresponding to the methylene (CD_2) symmetric stretching modes. Bands at 2177 and 2197 cm^{-1} are related to CD_2 asymmetric stretching modes, while the feature at 2215 cm^{-1} is assigned to the CD_3 asymmetric stretching modes (Bryant et al., 1982). By comparing panels A and B of Figure 2 (solid lines), we note that, as the phase of the DPPC-d_{62} bilayer changes from gel to liquid crystalline, both the 2103- and 2075-cm^{-1} bands broaden, with the feature at 2075 cm^{-1} becoming a shoulder. The line width of the 2103-cm^{-1} band determined at different peak heights has been shown to reflect differences in either the intermolecular or intrachain packing of deuterated lipids (Bryant et al., 1982). For example, increases in the $\Delta\nu_{7/8}$ line width reflect primarily an increase in the separation between lipid molecules and, therefore, provide a monitor of intermolecular bilayer disorder. Increases in the $\Delta\nu_{1/2}$ line width indicate primarily an increase in the number of gauche conformers along the lipid chains and, therfore, reflect an increase in intrachain disorder (Mendelsohn et al., 1976). As before, profiles of lipid packing dynamics can be constructed, in this case, by plotting the spectral line widths of the 2103-cm^{-1} band as a function of temperature. (The line widths reported in this paper are measured to ±0.5 cm^{-1}.)

In addition to the Raman spectra of pure DPPC-d_{62} bilayers, the Raman spectra of DPPC-d_{62} hydrated with a 126 mg/mL solution of ethanol are also displayed in Figure 2 (dashed lines). It has been previously demonstrated that this concentration of ethanol induces an interdigitated DPPC gel phase, similar to the interdigitated gel phase formed by DHPC (Rowe, 1985; Simon & McIntosh, 1984). This sample was examined spectroscopically as a control of the lipid dynamics of DPPC-d_{62} in an interdigitated phase. At 50 °C, there is very little difference between the Raman spectra of conventional DPPC-d_{62} bilayers and DPPC-d_{62} hydrated with 126 mg/mL ethanol (see Figure 2B), indicating that the morphology of the liquid-crystalline phase of DPPC-d_{62} is unaffected by ethanol. At 25 °C, the differences between the two Raman spectra are more evident (see Figure 2A). The peaks at 2075 and 2190 cm^{-1} become sharper, and the 2103-cm^{-1} band is narrowed for DPPC-d_{62} in the interdigitated phase. A detailed analysis of the effect of ethanol on the DPPC bilayer is currently being performed and will be reported at a later date. It is important, however, to note that changes in the line width of the 2103-cm^{-1} band are sensitive to changes in the packing of the gel phase of DPPC-d_{62} as well as to reorganizations of the bilayer arising as a result of liquid-crystalline phase formation.

Raman Spectra of Mixed DHPC/DPPC-d_{62} Bilayers. Representative Raman spectra of the various DHPC/DPPC-d_{62} mixtures studied here are displayed in Figures 3–5. Some general observations concerning the differences between these DHPC/DPPC-d_{62} mixtures and the pure DHPC and DPPC-d_{62} bilayers can be made from these spectra. Below the main phase transition of the mixed bilayers, DHPC becomes more disordered intermolecularly and intramolecularly as the mole percent of DPPC-d_{62} of the samples is increased (see panel A in Figures 3–5). The DHPC liquid-crystalline state also appears to become more disordered as the percent of DPPC-d_{62} in the samples is increased (see panel B in Figures 3–5). [For concentrations of >30 mol % DPPC-d_{62}, DHPC actually reorders (vide infra).] These conclusions are deduced from the decrease and increase, respectively, in the intensities of the C–H stretching mode features at 2880 and 2935 cm^{-1} relative to the intensity of the methylene symmetric stretching modes at 2850 cm^{-1}. Spectral examination of matrix effects indicates that the intensity pedestal upon which the 2880-cm^{-1} feature lies decreases in intensity as a consequence of reductions in the interchain vibrational coupling between nondeuterated hydrocarbon chains when they are isolated in a matrix of deuterated chains (Mendelsohn & Koch, 1980; Gaber & Peticolas, 1977; Snyder et al., 1978). Concomitant with the decrease in the intensity of the Fermi resonance background is a significant narrowing of the 2850- and 2880-cm^{-1} features (Snyder et al., 1978). These definitive spectral characteristics are not evident in panels A and B of Figures 3–5; therefore, we conclude that changes in the intensities of the C–H stretching modes of DHPC are indicative of changes in the packing of DHPC molecules and are not a result of an isotopic dilution of the nondeuterated DHPC chains. For DPPC-d_{62} the complimentary effects are seen in panels C and D of Figures 3–5. A decrease in the order of DPPC-d_{62} above and below the main phase transition is observed with decreases in the percent of DPPC-d_{62} in the mixed samples. This is indicated by an increase in the width of the 2103-cm^{-1} band measured at different peak heights.

Temperature Profiles Reflecting the Packing of DHPC/DPPC-d_{62} Mixed Bilayers. A more detailed examination of the packing dynamics of these samples can be made by examining the representative temperature profiles in Figures 6–9. The dashed lines in Figures 6 and 7 represent the temperature profiles for pure DPPC-d_{62} bilayers, while the dashed lines in Figures 8 and 9 represent the temperature profiles for pure DHPC bilayers. All other temperature profiles correspond to samples that are identified in the figure captions and whose lipid compositions are listed in Table I. As mentioned above, the temperature profiles in Figure 6, $\Delta\nu_{1/2}$ vs T, and Figure

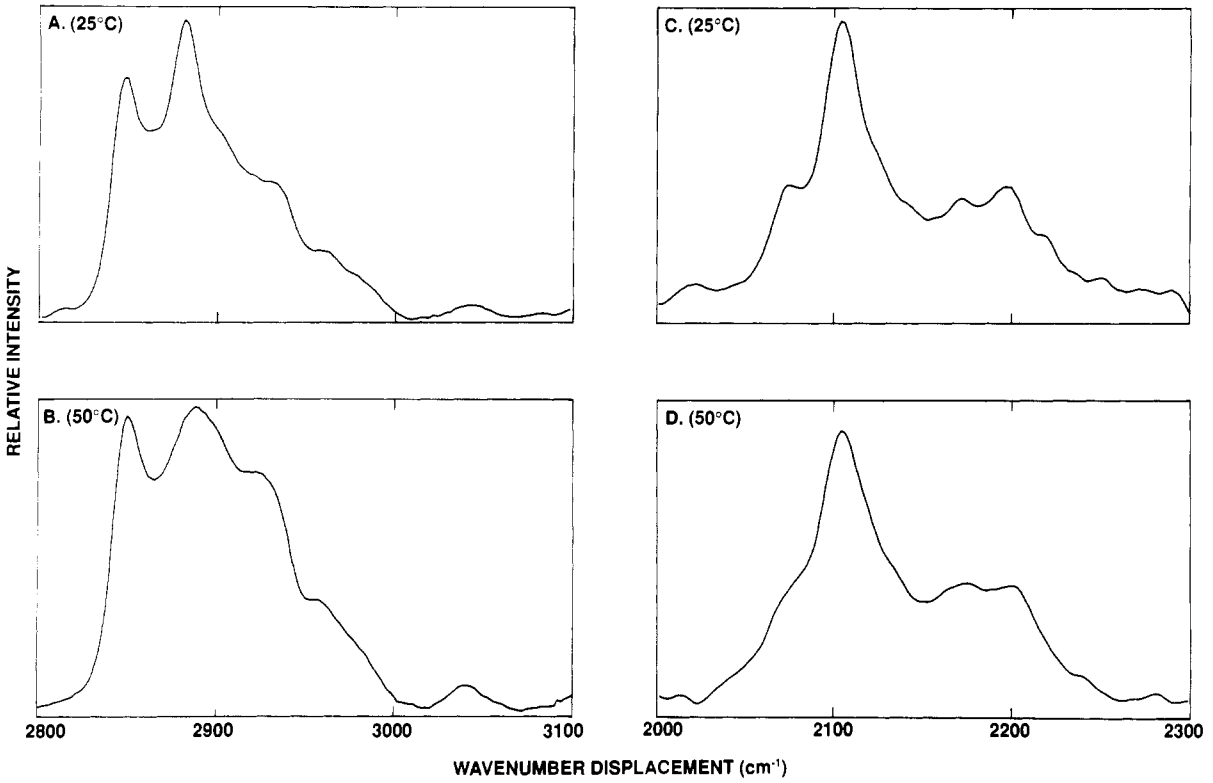

FIGURE 3: Raman spectra of the C–H stretching modes of DHPC (A and B) and the C–D stretching modes of DPPC-d_{62} (C and D) in a bilayer that contains 72 mol % DHPC and 28 mol % DPPC-d_{62}. Panels A and C are the Raman spectra of these lipids in the gel phase, and panels B and D are the Raman spectra of these lipids in the liquid-crystalline phase.

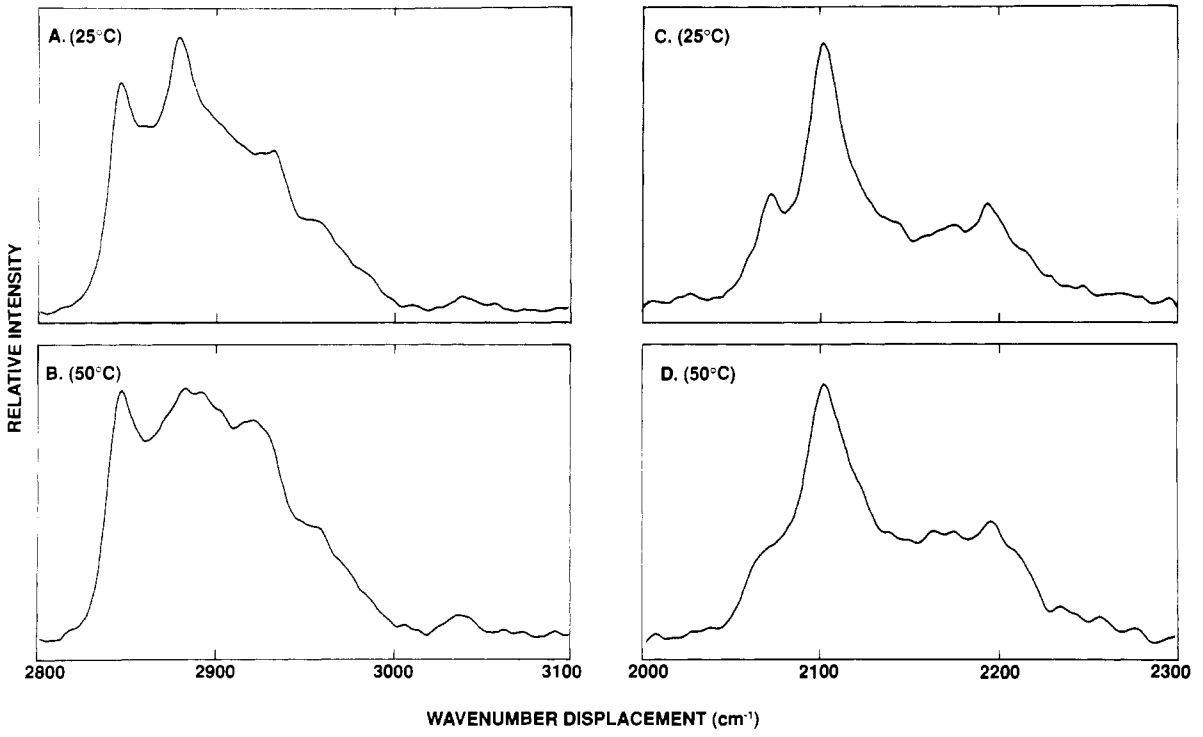

FIGURE 4: Raman spectra of the C–H stretching modes of DHPC (A and B) and the C–D stretching modes of DPPC-d_{62} (C and D) in a bilayer that contains 51 mol % DHPC and 49 mol % DPPC-d_{62}. Panels A and C are the Raman spectra of these lipids in the gel phase, and panels B and D are the Raman spectra of these lipids in the liquid-crystalline phase.

8, I_{2935}/I_{2880} vs T, represent changes in the intramolecular trans/gauche isomerization of the lipid chains superimposed upon changes in lateral intermolecular interactions, while the temperature profiles in Figure 7, $\Delta\nu_{7/8}$ vs T, and Figure 9, I_{2850}/I_{2880} vs T, represent primarily changes in the intermolecular order of the respective lipids. The data in Figure 8 demonstrate that as the mole percent of DPPC-d_{62} of the mixtures increases, the intramolecular disorder of the DHPC molecules increases. (The values for I_{2935}/I_{2880} increase.) This is true for the gel as well as liquid-crystalline phase. Additionally, the cooperative nature of the phase transitions is decreased with increases in the percent of DPPC-d_{62} in the mixtures, as indicated by the general increase in the transition width, ΔT, of the temperature profiles. The intermolecular

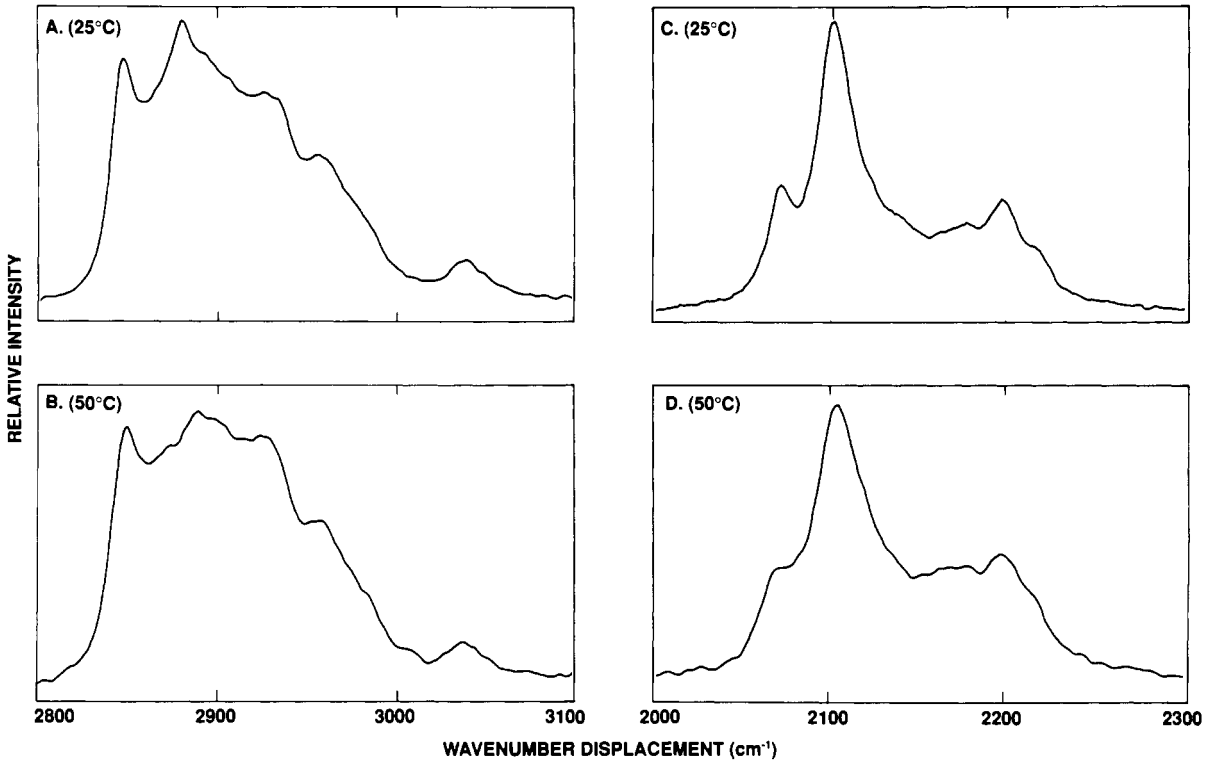

FIGURE 5: Raman spectra of the C–H stretching modes of DHPC (A and B) and the C–D stretching modes of DPPC-d_{62} (C and D) in a bilayer that contains 19 mol % DHPC and 81 mol % DPPC-d_{62}. Panels A and C are the Raman spectra of these lipids in the gel phase, and panels B and D are the Raman spectra of these lipids in the liquid-crystalline phase.

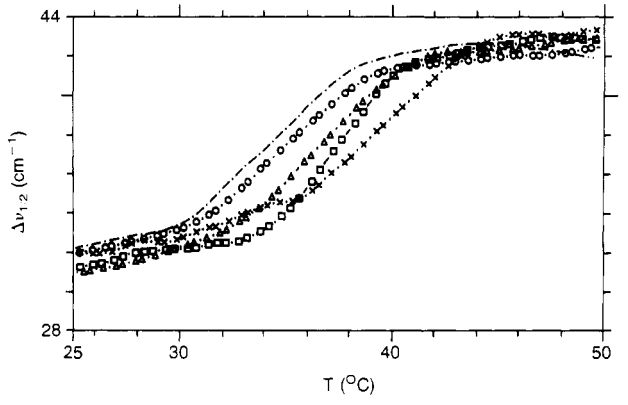

FIGURE 6: Temperature profiles showing the change in intramolecular order of DPPC-d_{62} in several different DHPC/DPPC-d_{62} mixed bilayers. The dashed line represents the temperature profile for a pure DPPC-d_{62} bilayer. The other symbols represent the temperature profiles for a variety of samples whose compositions are listed in Table I: (×) sample 1; (□) sample 3; (△) sample 5; (○) sample 6.

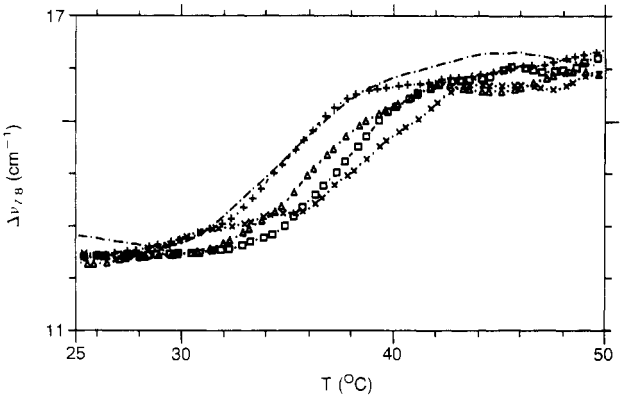

FIGURE 7: Temperature profiles showing the change in intermolecular order of DPPC-d_{62} in several different DHPC/DPPC-d_{62} mixed bilayers. The dashed line represents the temperature profile for a pure DPPC-d_{62} bilayer. The other symbols represent the temperature profiles for a variety of samples whose compositions are listed in Table I: (×) sample 1; (□) sample 3; (△) sample 5; (+) sample 7.

order of DHPC is quite different (see Figure 9). In the gel phase, DHPC molecules in all of the DHPC/DPPC-d_{62} mixtures have similar intermolecular order, as indicated by the values of the I_{2850}/I_{2880} peak height intensity ratios, but the mixed bilayers are more disordered than pure DHPC. Additionally, in the liquid-crystalline phase, DHPC molecules in samples 1–3 have the same intermolecular disorder as DHPC molecules in pure DHPC bilayers; however, as the percent of DPPC-d_{62} in the samples increases (in the samples with more then 30 mol % DPPC-d_{62}), the DHPC molecules become more ordered above T_m. When the concentration of DPPC-d_{62} is more than 90 mol %, the DHPC molecules are as ordered below the main phase transition as they are above the main phase transition. That is, the DHPC molecules appear to be trapped in a matrix of DPPC-d_{62} molecules, and for this concentration DHPC does not conform to DPPC-d_{62} bilayer changes occurring as a function of temperature.

A change in the composition of the mixed bilayers has no effect on the intramolecular and intermolecular order of DPPC-d_{62} away from the phase transition region (see Figures 6 and 7). The apparent packing differences shown in Figures 6 and 7 are negligible, since the error associated with all line widths is ±0.5 cm^{-1}. Clearly, the DHPC molecules in these mixed bilayers behave differently from the DPPC-d_{62} species. Therefore, in contrast to the previous DSC data presented for these mixed bilayers (Kim et al., 1987a; Lohner et al., 1987), the Raman data suggest that *DHPC and DPPC-d_{62} do not behave concertedly*, reflecting a lateral separation of the two species in the mixed bilayer. For a variety of mixed-lipid bilayers, it has been demonstrated that lateral segregation of lipids is not caused by the presence of a deuterated chain lipid analogue in the mixed bilayer (Laroche et al., 1988; Kouaouchi et al., 1985; Mendelsohn & Maisano, 1978; Mendelsohn & Taraschi, 1978). Therefore, the lateral separation detected

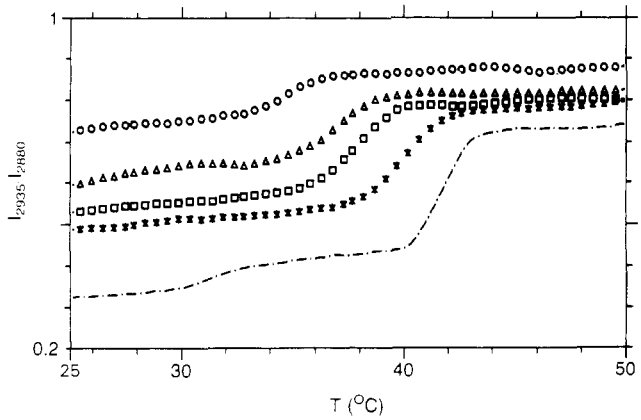

FIGURE 8: Temperature profiles showing the change in intramolecular order of DHPC in several different DHPC/DPPC-d_{62} mixed bilayers. The dashed line represents the temperature profile for a pure DHPC bilayer. The other symbols represent the temperature profiles for a variety of samples whose compositions are listed in Table I: (*) sample 2; (□) sample 3; (△) sample 5; (○) sample 6.

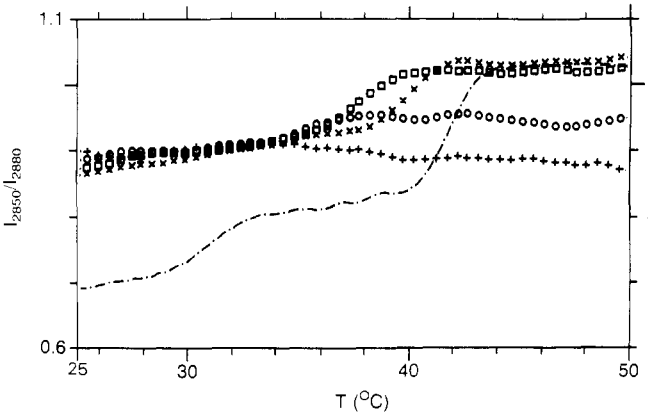

FIGURE 9: Temperature profiles showing the change in intermolecular order of DHPC in several different DHPC/DPPC-d_{62} mixed bilayers. The dashed line represents the temperature profile for a pure DHPC bilayer. The other symbols represent the temperature profiles for a variety of samples whose compositions are listed in Table I: (×) sample 1; (□) sample 3; (○) sample 6; (+) sample 7.

for the mixed DHPC/DPPC-d_{62} bilayers studied here is not a result of the technique employed to study these bilayers but, rather, is a result of the structural differences between DHPC and DPPC.

Table I summarizes all the thermodynamic data extracted from the Raman spectral data and from calorimetric measurements. The phase transition temperatures and phase transition widths in the last four columns are extracted from the temperature profiles shown in Figures 6–9, while the transition temperatures in the column labeled DSC are determined from DSC thermograms of the mixed bilayers (see Materials and Methods). [Since the nonlinear, least-squares fitting procedure employed for extracting the relevant thermodynamic information represents a statistically robust approach for obtaining these data (Kirchhoff & Levin, 1987), the T_m and ΔT values, listed in Table I and determined from the various spectral parameters discussed above, allow differences in the phase transition properties of the various samples to be discussed.] The transition temperatures (T_m) of each binary mixture, as determined from the Raman spectral data and DSC thermograms, reflect the same changes in bilayer packing properties that have been previously reported (Kim et al., 1987a; Lohner et al., 1987). As the mole percent of DPPC-d_{62} in the mixture is increased, the main phase transition temperature of the sample generally decreases. This trend occurs for both intermolecular (columns labeled 2850/2880 and $\Delta\nu_{7/8}$) and intramolecular (columns labeled 2935/2880 and $\Delta\nu_{1/2}$) bilayer characteristics of the DHPC and DPPC-d_{62} molecules. As the mole percent of DPPC-d_{62} in the samples is increased, the transition widths determined by DSC increase to a maximum of 3.4 °C for samples 3 and 4 and than decrease. However, except for occasional outliers, the trend for the phase transition widths for the DHPC molecules is toward a general increase (as indicated by the columns labeled 2850/2880 and 2935/2880), while the phase transition widths for the DPPC-d_{62} molecules tend to decrease (as indicated by the columns labeled $\Delta\nu_{7/8}$ and $\Delta\nu_{1/2}$).

Discussion

Both the intermolecular and intramolecular ordering of DHPC and DPPC-d_{62} within the mixed bilayer may be examined as a function of temperature, phase of each lipid, and composition of the DHPC/DPPC-d_{62} multilamellar samples. The general features of the packing dynamics of the mixed bilayers are discussed in terms of the phase diagram proposed for this mixed-lipid system by Kim et al. (1987a). X-ray diffraction studies have suggested that below the bilayer pretransition temperature two different gel phases may exist for the mixed DHPC/DPPC-d_{62} bilayers (Kim et al., 1987a). With less than 28 mol % DPPC in the mixtures the lipid chains in the gel phase are interdigitated, while above 50 mol % DPPC conventional bilayers are formed. Between 28 and 50 mol % DPPC, the phase diagram indicates that the two gel phases may coexist. The phase diagram also indicates that there exists only one ripple phase, namely, that in which the DHPC and DPPC molecules are homogeneously mixed. However, the results from the Raman Studies presented in this paper indicate that when the mixed bilayers are converted from the ripple gel phase to the liquid-crystalline phase, the two lipid species behave differently. This implies that the two lipid species are not homogeneously mixed and that separate pools of DHPC and DPPC-d_{62} may exist above the pretransition. Lohner et al., (1987) have shown that for DHPC/DPPC mixtures in the ripple phase, a discontinuity in the value of the bilayer repeat distance occurs. In the sample with 40 mol % DHPC the bilayer repeat distance of the ripple phase is approximately 70 Å, while at 50 mol % DHPC the repeat distance is approximately 78 Å. This suggests that two different ripple phases may be present in the mixed DHPC/DPPC bilayers and that the characteristics of these ripple phases depend upon the composition of the mixed bilayers.

Figures 6–9 illustrate the bilayer packing differences between DHPC and DPPC-d_{62} indicating a lateral separation of the lipids within the binary mixtures. As discussed under Results, except for a lowering of the T_m of the lipid assemblies, Figures 6 and 7 show that the packing characteristics of DPPC-d_{62} molecules are unaffected by the composition of the mixed bilayer. The DPPC-d_{62} molecules are aggregated, as indicated by the existence of a relatively broad phase transition. As measured by the transition width, ΔT (see Table I; columns labeled $\Delta\nu_{7/8}$ and $\Delta\nu_{1/2}$), the cooperativity of the main phase transition changes only slightly with reductions of the amount of DPPC-d_{62} in the mixtures. In contrast, variations in the composition of the mixed bilayers have a dramatic effect on the packing properties of DHPC molecules. Figure 9 shows that when the mixed bilayer contains only 11 mol % DHPC, no phase transition is detected for the DHPC molecules. Under these conditions either individual or small numbers of DHPC molecules may be considered to be trapped within assemblies of DPPC-d_{62} molecules which act to protect them from changes in lipid environment. As the mole percent of DHPC increases, phase transition behavior is detected for the

DHPC molecules in the binary mixtures. The cooperativity of this phase transition increases with increases in the mole percent of bilayer DHPC. This thermodynamic behavior is reflected by a general decrease in the phase transition widths, which are shown in Figures 8 and 9 (see also Table I, columns 2850/2880 and 2935/2880). In addition, the entropy of the observed DHPC phase transition increases as the percent of DHPC molecules in the mixed bilayer increases. The entropy changes are monitored by increases in the amplitudes of the temperature profiles derived from, particularly, the I_{2935}/I_{2880} parameters (see Figure 9) (Huang et al., 1982). These bilayer characteristics provide evidence for the aggregation of DHPC molecules to form pools or domains. If DHPC molecules were homogeneously mixed or freely associated with DPPC-d_{62} molecules, the behavior of the DHPC molecules in mixed bilayers with less than 50 mol % DHPC would be similar to that of the DPPC-d_{62} molecules in these mixtures. Also, we would expect the DHPC molecules to behave analogously to the DHPC molecules in the 11 mol % DHPC mixed bilayer in which no ether lipid phase transition is observed. If, however, DHPC molecules move from a domain associated with DPPC-d_{62} to a more intramolecularly ordered DHPC domain, the cooperative nature and entropy of the phase transition for all DHPC molecules would increase, as observed. In summary, Figures 6–9 demonstrate that DPPC-d_{62} and DHPC molecules reflect bilayer behavior consistent with existence of segregated lipid pools within the binary mixtures.

Further examination of the Raman temperature profiles of the DHPC/DPPC-d_{62} mixtures enables us to determine in greater detail the intermolecular and intramolecular ordering of the DHPC and DPPC-d_{62} molecules within the various putative lipid domains. First, however, we identify for the binary mixtures three possible lipid classes, namely, separate domains for each bulk species and the interfacial, or boundary, domains between them. For each lipid species the derived order/disorder parameters, which provide the bilayer phase transition temperatures and transition widths, reflect spectral contributions averaged over both the bulk and interfacial domains. The phase transition behavior of the bulk lipid domains may be similar to the characteristics of pure lipid bilayers, but the behavior of the interface domains will be critically dependent upon their composition, which is a function of the relative mole fractions of the entire mixed bilayer. That is, for the interface domains containing a disproportionate amount of either lipid, the resulting phase behavior would be characteristic of this specific mixture of ether-linked and acyl-linked molecules. As a result, differences in the phase transtion behavior of DHPC and DPPC-d_{62} molecules would not be strictly reflected in the phase transition temperatures determined for the two lipid species, since the transition profiles and, thus, the phase transition temperatures would be representative of the composition of the interfacial domains. Despite this, characteristics of the three domains can be discerned by examining changes in the spectral order parameters as a function of sample composition. For example, as the composition of DPPC-d_{62} in the mixed bilayers is increased, the number and size of the bulk DPPC-d_{62} domains increase at the expense of interfacial DPPC-d_{62} molecules. Raman spectra of these samples would be more characteristic of bulk-phase DPPC-d_{62} molecules than of DPPC-d_{62} molecules participating in the boundary regions. Conversely, the Raman spectra of binary mixtures with low DPPC-d_{62} mole fractions should be more characteristic of DPPC-d_{62} molecules within the interfacial domains. This same reasoning may be applied to the DHPC molecules for the various mixed bilayers.

The intramolecular and intermolecular ordering of DPPC-d_{62} molecules in the mixed bilayers are compared in Figures 6 and 7. For the gel, ripple, and liquid-crystalline phases, a change in the composition of the mixed bilayers does not alter significantly either the number of gauche conformers along the DPPC-d_{62} chains or their lateral interactions. Thus, the samples containing a high percent of DPPC-d_{62}, characteristic of DPPC-d_{62} molecules primarily in the bulk DPPC-d_{62} domains, have the same inter- and intrachain order as the samples comprised of a low mole percent of DPPC-d_{62}, representative of DPPC-d_{62} molecules being located mostly in boundary domains. Since there is essentially no change in either the interchain or intrachain order of DPPC-d_{62} molecules as a function of sample composition, we conclude that the DPPC-d_{62} molecules are packed in the same general manner in both the bulk and interfacial DPPC-d_{62} domains.

The uniform packing characteristics of DPPC-d_{62} molecules in the mixed bilayers is contrasted by the sensitivity of DHPC to its lipid environment. Figure 8 reflects the intramolecular ordering of DHPC molecules in the bulk and the interfacial domains. As the percent of DHPC in the mixed samples decreases, the intramolecular order of the gel, ripple, and liquid-crystalline states of DHPC decreases. This disorder can be related to a decrease in the number of DHPC molecules in the bulk DHPC domain. Since the ether-linked hydrocarbon chains of the DHPC molecules in the ripple phase are expected to pack more tightly than the acyl chains of DPPC, the number of intrachain gauche conformers is expected to be minimized in the bulk domain. In the interfacial domain, however, DHPC molecules are more loosely packed as a result of their interactions with DPPC-d_{62} molecules; thus, more gauche conformers would be induced. As the mole percent of DHPC in the binary mixtures decreases, reducing the size of the bulk DHPC domains, the observed Raman signal averaged over the entire population of hydrocarbon chains will reflect an increase in the number of DHPC gauche conformers. Figure 9 shows that gel and ripple phase DHPC has the same intermolecular order regardless of sample composition; however, these molecules exhibit significantly decreased intermolecular interactions in contrast to pure DHPC in the interdigitated gel and ripple phases. This suggests that the presence of DPPC-d_{62} in the mixed bilayer determines the chain–chain interactions of the DHPC domains by perturbing the order of DHPC molecules in the interfacial domain. That is, interfacial DHPC molecules are perhaps predisposed to form a given intermolecular orientation dictated by interactions from neighboring interfacial DPPC-d_{62} molecules. This is demonstrated for sample 7 (11 mol % DHPC) by the absence of a phase transition derived from parameters associated with the intermolecular interactions (see Figure 9).

The uniformity of the DPPC-d_{62} packing properties and the more variable packing dynamics of DHPC may be related to differences in lipid-chain mobility stemming from either the ester or ether linkage near the lipid headgroup regions. NMR studies have shown that axial diffusion of DHPC persists to lower temperatures than axial diffusion of DPPC-d_{62} (Ruocco et al., 1985; Davis, 1979). This suggests that the acyl linkage of DPPC-d_{62} stabilizes the packing arrangements of the DPPC-d_{62} bilayer or domain. [These stabilizing interactions may include hydrogen-bonding interactions involving the ester linkage of DPPC-d_{62} (Boggs, 1987).] As the composition of the domains in the bilayer other than DPPC-d_{62} change, the intermolecular and intramolecular characteristics of the bulk DPPC-d_{62} domain (at a given temperature) would tend to be invariant. The presence of an ether linkage, in contrast, results

in an enhanced rotational diffusion for the DHPC species and in an increased molecular flexibility near the ether-linked headgroup. Due to the loss of hydrogen-bonding interactions involving the lipid headgroup and interfacial regions, the predominant stabilizing force for DHPC molecules in the bulk and interfacial domains is the van der Waals contacts between DHPC chains. In order to maximize these contacts, DHPC molecules would conform to the packing characteristics of the other components in the bilayer.

Conclusions

The Raman spectral data indicate that DHPC and DPPC-d_{62} do not act concertedly in mixed DHPC/DPPC-d_{62} bilayers. A model consistent with these data involves laterally separated bulk DHPC and DPPC-d_{62} domains, as well as boundary regions containing both lipid species. For the mixed bilayers we note that the lipid dynamics of DPPC are invariant to the lipid composition of the system. We attribute this to a conferred intermolecular and intramolecular stability by the acyl linkage in DPPC-d_{62}. The presence of the ether linkage in DHPC results in variable lipid dynamics. Since DHPC molecules are both more flexible and more mobile, variations in interchain and intrachain interactions occur. As a result of the different lipid dynamics of DHPC and DPPC-d_{62}, it is reasonable to expect DHPC to be better suited for interacting with other bilayer constituents without affecting the membrane's overall packing properties.

References

Albert, D. H., & Anderson, C. E. (1977) *Lipids 12*, 188–192.

Boggs, J. M. (1987) *Biochim. Biophys. Acta 906*, 353–404.

Boyanov, A. I., Tenchov, B. G., Koynova, R. D., & Koumanov, K. S. (1983) *Biochim. Biophys. Acta 732*, 711–713.

Boyanov, A. I., Koynova, R. D., & Tenchov, B. G. (1986) *Chem. Phys. Lipids 39*, 155–163.

Bryant, G. J., Lavialle, F., & Levin, I. W. (1982) *J. Raman Spectrosc. 12*, 118–121.

Bunow, M. R., & Levin, I. W. (1977) *Biochim. Biophys. Acta 489*, 191–206.

Davis, J. H. (1979) *Biophys. J. 27*, 339–358.

Gaber, B. P., & Peticolas, W. L. (1977) *Biochim. Biophys. Acta 465*, 260–274.

Goldfine, H., Johnston, N. C., Mattai, J., & Shipley, G. G. (1987) *Biochemistry 26*, 2814–2822.

Gross, R. W. (1984) *Biochemistry 23*, 158–165.

Huang, C.-H., Lapides, J. R., & Levin, I. W. (1982) *J. Am. Chem. Soc. 104*, 5926–5930.

Kim, J. T., Mattai, J., & Shipley, G. G. (1987a) *Biochemistry 26*, 6599–6603.

Kim, J. T., Mattai, J., & Shipley, G. G. (1987b) *Biochemistry 26*, 6592–6598.

Kirchhoff, W. H., & Levin, I. W. (1987) *J. Res. Natl. Bur. Stand. 92*, 113–128.

Kouaouchi, R., Silvius, J. R., Graham, I., & Pézolet, M. (1985) *Biochemistry 24*, 7131–7140.

Laggner, P., Lohner, K., Degovics, G., Müller, K., & Schuster, A. (1987) *Chem. Phys. Lipids 44*, 31–60.

Laroche, G., Carrier, D., & Pézolet, M. (1988) *Biochemistry 27*, 6220–6228.

Levin, I. W. (1984) *Adv. Raman Spectrosc. 11*, 1–49.

Lohner, K., Schuster, A., Degovics, G., Müller, K., & Laggner, P. (1987) *Chem. Phys. Lipids 44*,, 61–70.

Mangold, H. K., & Paltauf, F. (1983) *Ether Lipids: Biochemical and Biomedical Aspects*, Academic Press, New York.

Mendelsohn, R., & Maisano, J. (1978) *Biochim. Biophys. Acta 506*, 192–201.

Mendelsohn, R., & Taraschi, T. (1978) *Biochemistry 17*, 3944–3949.

Mendelsohn, R., & Koch, C. C. (1980) *Biochim. Biophys. Acta 598*, 260–271.

Mendelsohn, R., Sunder, S., & Bernstein, H. J. (1976) *Biochim. Biophys. Acta 443*, 613–617.

Petersen, N. O., Kroon, P. A., Kainosho, M., & Chan, S. I. (1975) *Chem. Phys. Lipids 14*, 343–349.

Rowe, E. S. (1985) *Biochim. Biophys. Acta 813*, 321–330.

Ruocco, M. J., Siminovitch, D. J., & Griffin, R. G. (1985) *Biochemistry 24*, 2406–2411.

Sakurai, I., Sakurai, T., Seto, T., & Iwayanagi, S. (1983) *Chem. Phys. Lipids 32*, 1–11.

Simon, S. A., & McIntosh, T. J. (1984) *Biochim. Biophys. Acta 773*, 169–172.

Snyder, R. G., Hsu, S. L., & Krimm, S. (1978) *Spectrochim. Acta 34A*, 395–406.

Tenchov, B. G., Boyanov, A. I., & Koynova, R. D. (1984) *Biochemistry 23*, 3553–3558.